PRIFYSGOL ABERYSTWYTH UNIVERSITY

Aberystwyth University

Chute cutoff-driven abandonment and sedimentation of meander bends along a fine-grained, non vegetated, ephemeral river on the Bolivian Altiplano

Li, Jiaguang; Grenfell, Michael C.; Wei, Hao; Tooth, Stephen; Ngiem, Sophea

Published in:
Geomorphology

DOI:
10.1016/j.geomorph.2019.106917

Publication date:
2020

Citation for published version (APA):
Li, J., Grenfell, M. C., Wei, H., Tooth, S., & Ngiem, S. (2020). Chute cutoff-driven abandonment and sedimentation of meander bends along a fine-grained, non vegetated, ephemeral river on the Bolivian Altiplano. *Geomorphology*, *350*, [106917]. https://doi.org/10.1016/j.geomorph.2019.106917

General rights
Copyright and moral rights for the publications made accessible in the Aberystwyth Research Portal (the Institutional Repository) are retained by the authors and/or other copyright owners and it is a condition of accessing publications that users recognise and abide by the legal requirements associated with these rights.

• Users may download and print one copy of any publication from the Aberystwyth Research Portal for the purpose of private study or research.
• You may not further distribute the material or use it for any profit-making activity or commercial gain
• You may freely distribute the URL identifying the publication in the Aberystwyth Research Portal

Take down policy
If you believe that this document breaches copyright please contact us providing details, and we will remove access to the work immediately and investigate your claim.

tel: +44 1970 62 2400
email: is@aber.ac.uk

Download date: 06. May. 2023

Journal Pre-proof

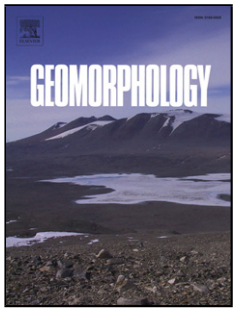

Chute cutoff-driven abandonment and sedimentation of meander bends along a fine-grained, non-vegetated, ephemeral river on the Bolivian Altiplano

Jiaguang Li, Michael C. Grenfell, Hao Wei, Stephen Tooth, Sophea Ngiem

PII: S0169-555X(19)30408-8

DOI: https://doi.org/10.1016/j.geomorph.2019.106917

Reference: GEOMOR 106917

To appear in:

Received Date: 6 July 2019

Revised Date: 21 October 2019

Accepted Date: 21 October 2019

Please cite this article as: Li J, Grenfell MC, Wei H, Tooth S, Ngiem S, Chute cutoff-driven abandonment and sedimentation of meander bends along a fine-grained, non-vegetated, ephemeral river on the Bolivian Altiplano, *Geomorphology* (2019), doi: https://doi.org/10.1016/j.geomorph.2019.106917

This is a PDF file of an article that has undergone enhancements after acceptance, such as the addition of a cover page and metadata, and formatting for readability, but it is not yet the definitive version of record. This version will undergo additional copyediting, typesetting and review before it is published in its final form, but we are providing this version to give early visibility of the article. Please note that, during the production process, errors may be discovered which could affect the content, and all legal disclaimers that apply to the journal pertain.

© 2019 Published by Elsevier.

Journal Pre-proof

Chute cutoff-driven abandonment and sedimentation of meander bends along a fine-grained, non-vegetated, ephemeral river on the Bolivian Altiplano

Jiaguang Li[1]*, Michael C. Grenfell[2], Hao Wei[1], Stephen Tooth[3], Sophea Ngiem[1]

[1] Key Laboratory of Tectonics and Petroleum Resources of the Ministry of Education, China University of Geosciences, Wuhan, 430074, China (jiaguanglicn@yahoo.com, jiaguangli@gmail.com)

[2] Institute for Water Studies, Department of Earth Science, University of the Western Cape, Bellville, South Africa

[3] Department of Geography and Earth Sciences, Aberystwyth University, Aberystwyth, SY23 3DB, UK

Highlights

- we present an analysis of chute cutoff along a non-vegetated, ephemeral river
- twenty-two cutoffs are evident, with chute cutoff the dominant mechanism
- chute cutoffs occur despite low stream powers (<10 W/m^2) and cohesive sediments
- episodic La Niña-driven flood events drive clusters of chute cutoffs
- findings contribute to improved understanding of dryland river meander dynamics

Abstract

The origin and development of meandering river planforms has long been a focus of research in the geosciences. Most attention has focused on perennial meandering rivers with well developed riparian vegetation assemblages, and while increasing interest is turning towards the dynamics and sedimentology of ephemeral meandering rivers with sparse to no vegetation, additional field data

Journal Pre-proof

Journal Pre-proof

are required. As a contribution, this study presents a remote-sensing and field-based analysis of chute cutoff-driven abandonment and sedimentation of meander bends along the fine-grained, non-vegetated, ephemeral Río Colorado on the Bolivia Altiplano. Along the 25 km long sinuous study reach, located between 25 and 50 km upstream of the present-day margins of Salar de Uyuni, quasi-regular flood events (typically at least one per year) drive bend cutoffs and wider channel-floodplain dynamics, despite low specific stream power (<10 W/m^2) and cohesive (dominantly silt and clay) bed and bank sediments. Along the reach, twenty-two cutoffs are evident, with chute cutoff the dominant mechanism. Three chute cutoffs (CC1, CC2, CC3) occurred between 1996 and 2016; for one bend (CC3), high-resolution (<0.65 m) satellite imagery and field investigations reveal the details of pre-, mid- and post-chute cutoff processes and sedimentary products. Together, the findings suggest that for any given bend, an increase in bend amplitude (mean ratio of meander bend length to chute channel length ~4) combines with a typically high diversion angle between the channel-belt axis and the upstream limb of the meander bend (mean ~98°) to result in declining flow efficiencies. This enhances overbank flooding and promotes deposition along the upstream limb of the bend. Overbank flooding promotes the development of chute channels, which commonly initiate as shallow (typically <1 m) headward eroding channels, while sediment derived from overbank flow and headward erosion tends to be deposited in the downstream limb of the bend. By obstructing flow, such

Journal Pre-proof

deposition reduces sediment transport capacity within the meander bend as a whole, thereby further inducing deposition within the upstream limb. During subsequent floods, deepening and widening of a dominant chute channel and sedimentation and shallowing of the meander bend continues. Along the reach, episodic La Niña-driven flood events drive phases of more rapid bend migration and clusters of chute cutoffs. Our findings contribute to a more comprehensive understanding of meandering river dynamics across the full range of Earth's conditions, and also may help to improve interpretations of Earth's pre-vegetation rivers and meandering fluvial forms on other planetary bodies.

Keywords: chute channel, chute cutoff, dryland river, ephemeral, meandering, non-vegetated

Introduction

Through the use of field investigations, aerial image analyses, flume-based experiments and computational modelling approaches, the forms, processes and sedimentological implications of meander bend cutoffs have been intensively studied (e.g., Fisk, 1944, 1947; Lewis and Lewin, 1983; Gagliano and Howard, 1984; Hooke, 1995, 2004; Stølum, 1996, 1998; Peakall et al., 2007; Constantine and Dunne, 2008; Zinger et al., 2011; Schwenk and Foufoula-Georgiou, 2016). Cutoffs greatly influence channel-floodplain geomorphology, hydraulics and sedimentology, and have implications for interpretations and economic exploration of meandering systems preserved in

Journal Pre-proof

Journal Pre-proof

the rock record, with sandy channel fills in particular commonly forming alluvial aquifers or hydrocarbon reservoirs (Miall, 1996; Bridge, 2003; Ghinassi et al., 2018). Two main cutoff types (end members) have been defined: neck cutoff and chute cutoff. Neck cutoffs occur when maturing meander bends migrate into one another owing to progressive riverbank erosion. Chute cutoffs are associated with chute channel development that typically results from one or a combination of three main processes (see Grenfell et al., 2012): (i) erosion of swales or other topographic lows by headward eroding channels (headcuts) across the inner meander bend surface; (ii) headward erosion from the downstream meander limb, coupled with bank erosion at the upstream limb (Constantine et al., 2010b; Zinger et al., 2011; Grenfell et al., 2012; van Dijk et al., 2012); and (iii) distinct from the aforementioned incisional mechanisms, deposition of a mid-channel bar around a bend, with the inner channel branch gradually assuming dominance (Bridge et al., 1986). Chute cutoffs by headward eroding channels have been widely attributed to natural dams that locally force overbank flooding (e.g., woody debris or ice jams – Keller and Swanson, 1979; Gay et al., 1998; Smith and Pearce, 2002), although the development of headward eroding channels at points of overbank flow re-entry can occur without active damming upstream (Hooke, 1995; Gay et al., 1998).

Field studies of meander dynamics have investigated both neck and chute cutoffs, in some cases with both cutoff types occurring along a given study reach or river (e.g., Lewis and Lewin, 1983; Hooke, 1995). Such studies have

Journal Pre-proof

tended to focus mainly on moderate to high energy, sand- and gravel-bed, perennial rivers where bankline and floodplain vegetation is typically well developed. By contrast, and despite a recent rise in interest in meander dynamics in dryland rivers (e.g., Billi et al., 2018; Santos et al., 2019) detailed studies of cutoffs in lower energy, fine-grained, ephemeral rivers with sparsely vegetated or non-vegetated banks and floodplains are rarer (see Ielpi, 2018; Ielpi and Lapôtre, 2019). Furthermore, computational modelling studies have focused largely on neck cutoffs, primarily owing to the difficulties associated with coding chute cutoff rules into commonly used 1D numerical simulation schemes. These gaps in knowledge limit our ability to develop more comprehensive theories of meander bend development and wider channel planform dynamics.

Against this backdrop, field and remote sensing investigations of chute cutoffs occurring in low-energy meandering rivers in the absence of vegetation can provide new geomorphological and sedimentological insights, particularly where cutoff development is occurring over observable timescales (i.e., years to decades). To exploit these opportunities, this study investigates chute cutoff-driven abandonment and sedimentation of meander bends along the fine-grained, non-vegetated, ephemeral Río Colorado approaching its terminus on the margins of Salar de Uyuni, Bolivia, the world's largest salt lake (Fig. 1). Previous studies of the middle and lower reaches of the Río Colorado and neighbouring rivers have revealed the widespread, pronounced

Journal Pre-proof

Journal Pre-proof

channel-floodplain dynamics that result from quasi-regular (typically at least once a year) within-channel and overbank flooding (Li, 2014; Li et al., 2014a; Li et al., 2018) and have drawn preliminary comparisons with the morphodynamics of non-vegetated rivers in similar physiographic contexts worldwide, including in North America and Asia (e.g., Li et al., 2019). While some of the previous studies on the Río Colorado have noted chute cutoffs that occur as part of meander-belt development and wider cascades of channel-floodplain changes (e.g., Li et al., 2019), the geomorphological, hydraulic or sedimentary processes of cutoffs have not been investigated in any detail. Our study aims to: (1) use satellite imagery, hydraulic modelling and field investigations to document the processes of chute cutoff-driven abandonment and sedimentation of meander bends; (2) interpret the key flow and sediment controls of chute cutoff development in this setting; and (3) compare the processes of chute cutoff development along the Río Colorado with the dynamics of other meandering rivers, including rivers with perennial flow regimes and greater vegetative influences.

1. Regional setting

The Río Colorado catchment lies within the southern part of the intra-continental Altiplano basin (Fig. 1A, B), which formed as part of the Andean oceanic-continental convergent margin. The Altiplano basin is filled with Tertiary to Quaternary fluvial and lacustrine sediments and volcaniclastic

Journal Pre-proof

deposits (Horton and Decelles, 2001; Elger et al., 2005). The Río Colorado catchment comprises upper Ordivician to Tertiary clastic sedimentary and igneous rocks, with Quaternary sediments widespread (Marshall et al., 1992; Horton and Decelles, 2001). Despite some prominent fault escarpments in the catchment (Bills et al., 1994; Baucom and Rigsby, 1999; Rigsby et al., 2005; Donselaar et al., 2013), the region has been tectonically quiescent in the late Pleistocene and Holocene.

The Río Colorado flows south-north, terminating at the southeastern margin of Salar de Uyuni (Fig. 1B). Previous studies have focused mainly on the fan-shaped lower reaches approaching the terminus (Donselaar et al., 2013; Li et al., 2014a,b, 2015b, 2018, 2019; Li and Bristow, 2015; van Toorenenburg et al., 2018) and also have investigated the anabranching morphodynamics on the nearby Río Capilla (Li et al., 2015a). In this study, greater attention is focused on a 25 km long reach of the Río Colorado located between 25 and 50 km upstream of the margins of Salar de Uyuni (Fig. 1B, C).

The Altiplano has a dryland climate, with a prominent decrease in aridity index (United Nations Environment Programme, 1992) from ~0.5 in the north (dry subhumid/semiarid) to ~0.12 in the south (Lenters and Cook, 1999). The region is subject to the influence of the El Niño Southern Oscillation (ENSO); consequently, annual rainfall in the study area is highly variable but averages ~185 mm and the 24 hour maximum daily precipitation only rarely exceeds 40 mm (Li, 2014; Li and Bristow, 2015). Annual precipitation is greatly exceeded

Journal Pre-proof

by the annual potential evapotranspiration of 1500 mm. As a consequence, the Río Colorado is ephemeral with river flow occurring mainly in response to thunderstorms in the austral summer (December through March - Li et al., 2014a). Although there are no formal flow gauging records, previous observations indicate that small to moderate (sub-bankfull) river flow events occur one or more times in most years, with larger events (bankfull or above) occurring at least once every few years (Li et al., 2018; Li et al., in prep). Field data on sediment loads are limited, but grain-size analyses indicate that the lower Río Colorado system is dominated by silt and clay with subordinate very fine sand (Li et al., 2015a). In the lowermost reaches approaching the terminus, channel-belt sediments are prograding over older (pre-late Holocene) lacustrine muds (Donselaar et al., 2013; Li et al., 2018). These fine-grained sediments, coupled with local salt cementation, contribute to the cohesion of bed, bank and floodplain surfaces. Normalized Difference Vegetation Index (NDVI) analysis and field observations indicate that the middle to lower reaches and terminus of the Río Colorado are essentially non-vegetated owing to the characteristically dry and saline environment (Li et al., 2015a).

2. Methods

Our study used a combination of data derived from remote sensing image analyses, precipitation analyses and discharge modelling, and field measurements and sampling.

Journal Pre-proof

Journal Pre-proof

3.1. Remote sensing analyses

Various satellite image datasets were used in this study to investigate channel planform dynamics. These included Landsat (1975-2011), Advanced Spaceborne Thermal Emission and Reflection (ASTER, 2000-2013), and high-resolution imagery (QuickBird02, WorldView02, Pléiades, 2004-2018, Table 1). Initially, the Landsat imagery was used to identify chute cutoff events that have taken place along the study reach over the last 40-45 years. Subsequently, the moderate resolution ASTER imagery and the high-resolution (<0.65 m) QuickBird02, WorldView02 and Pléiades imagery were used to visualize in greater detail the spatiotemporal development of chute cutoffs and post-chute cutoff meander bend sedimentation during the last two decades. Guided by data availability and quality, a 6.5 km long reach was selected for particular analysis over this more recent timeframe (Fig. 1C; see location of Figs. 3 and 4). Newer high-resolution images were registered to the reference image of 2004 using the remote sensing image analysis software ENVI. Along with field measurements (see below), these satellite images were used to quantify a range of channel parameters, including bankfull channel width.

3.2. Precipitation analyses and discharge modelling

Daily precipitation data for the period 1978 to 2016 were obtained for two monitoring stations in the Río Colorado catchment from the Bolivian Servicio

Journal Pre-proof

Nacional de Meteorología e Hidrología (http://www.senamhi.gob.bo/). These data were used for calculating average catchment area precipitation using the Thiessen Polygon method. Catchment parameters such as catchment area and slope were derived from Digital Elevation Model (DEM) data by Advanced Land Observation Satellite Phased Array type L-band Synthetic Aperture Radar (ALOS PALSAR) with a spatial resolution of 12.5 m (https://www.asf.alaska.edu/). Along with these parameters and some field measurments (see below), daily precipitation data were used for discharge modelling based on the model by El-Hames (2012). Rainfall events in the catchment area are widespread and well represented by the gauge locations (Li et al., 2014b).

3.3. Field measurements and sampling

To complement the remote sensing interpretations, precipitation analyses and discharge modelling, fieldwork was undertaken in November 2015. The field campaign deployed a Trimble R7 dual frequency geodetic Global Positioning System to retrieve high-precision elevation data and thus quantify downvalley gradients in the study area (see Li et al. (2015b) for details on data processing). The aforementioned datasets were used as input for discharge modelling using the El-Hames (2012) model to derive a catchment-scale daily discharge in the study area (see Li et al., 2014a). In specific meander bends and cutoffs, channel depths were measured using a tape measure and laser

Journal Pre-proof

range finder, and satellite-derived bankfull channel width measurements provided a basis for calculating bankfull discharge using Bjerklie's (2007) model, as well as the associated specific stream power.

Sedimentological investigations focused on one particular chute channel and cutoff (termed chute channel 3 (CC3) – see Fig. 1C). Four trenches in the channel fills and accretionary bars were logged and sampled. Trench depths were about 1 m with sampling intervals at 0.1 m. Samples were subsequently sent to the China University of Geosciences (CUG) laboratory for grain-size distribution analyses. Removal of organic matter and calcium carbonate (see details in Konert and Vandenberghe, 1997) preceded analysis using a laser-diffraction particle sizer with a size range from 0.1 to 2000 μm.

3. Results

River meanders formed in the absence of vegetative influences are considered to be 'exceptional' on modern Earth (Ielpi, 2018) but are common along the middle and lower reaches of the low energy, fine-grained, non-vegetated Río Colorado. Active development of many of these bends provides a rare opportunity to document in detail the processes of chute cutoff-driven abandonment and sedimentation of meander bends.

4.1. Channel planform dynamics

Landsat imagery indicates that the study reach has experienced two major

Journal Pre-proof

Journal Pre-proof

avulsions over the last 40-45 years (Fig. 2). The 1975 Landsat MSS image shows that the trunk channel was located on the western side of the valley (Fig. 2, reaches A and B) and characterized by a moderate sinuosity index (P = 1.94, where P = channel distance/straight-line distance), whereas a secondary channel on the eastern side (Fig. 2, reaches C and D) was relatively straight (P = 1.13) and appears to have been less active. The 1985 Landsat TM image shows that both the western and eastern channels were simultaneously active, thus forming an anabranching pattern. The 1996 Landsat image shows that the western channel had been largely abandoned in favour of the more eastern channel but with some flow still being diverted from the middle reach of the eastern channel through crevasse channels to the downstream part of the western channel (Fig. 2). The 2001 Landsat imagery shows that this flow diversion resulted in another avulsion that reoccupied the middle and downstream part of the western channel (Fig. 2, reaches C and B), although the eastern channel remained partially active. This planform has remained essentially the same from 2001 to present, although the eastern channel has experienced more dynamism with a couple of minor avulsions occurring in the downstream section. At present, the trunk (western) channel has a sinuosity index of 1.27. Channel width ranges from 20 to 30 m, and field measurements reveal that average depth is ~1.3 m (n = 15, range 1.0 to 1.65 m), so the mean width-depth ratio is about 20. In many locations, well developed scroll bar sets are evident on the inner bends; changes in the orientation of the scroll

Journal Pre-proof

bars indicate different modes of bend migration during the lifetime of some individual bends, including extension, translation and rotation (Jackson II, 1976). Between 2004 and 2016, the mean lateral migration rate for many bends was ~1 m/yr, with a maximum rate of 2.58 m/yr.

Satellite imagery reveals that a total of 22 cutoffs have occurred along the presently active and abandoned channels in the study reach (Fig. 1C). Although a component of meander neck erosion cannot be ruled out, the relatively open bends suggest that in all cases bend abandonment appears to have occurred mainly through chute cutoff development. For these 22 cutoffs, the mean ratio of the length of the abandoned bend to the length of chute channel is 4 (Table 2). The mean diversion angle between the channel-belt axis with its associated chute channel and the upstream limb of the abandoned bend (Constantine et al., 2010a) is 98° (Table 2). ASTER satellite imagery shows that three of these 22 chute cutoffs have occurred in recent decades, with cutoff completion dates occurring between 1997-1999, 2000-2002 and 2010-2013 (Fig. 3). These three chute cutoffs have been numbered in chronological sequence (Figs. 1C, 2 and 3): chute cutoff 1 (CC1), chute cutoff 2 (CC2) and chute cutoff 3 (CC3).

To document chute cutoff development in detail, our study focused on CC3. For this cutoff, high-resolution (<0.65 m) satellite imagery and ground level photographs from 2004 to 2018 covers the full suite of cutoff processes

Journal Pre-proof

(pre-chute cutoff, chute cutoff, and post-chute cutoff) (Figs. 4 and 5), whereas for CC1 and CC2 only the post-cutoff processes are observable in high resolution satellite imagery (Fig. 6).

4.1.1. Pre-chute cutoff

The 2004 high resolution imagery shows that there was a sinuous channel (~140 m long) across the meander neck that connected the upstream and downstream limbs of the bend (Fig. 4A, G). This channel was wide (up to 30 m) for the first 80 m, but became narrower downstream (~2 m wide), and is geometrically similar to the type of embayment channel described by Constantine et al. (2010). On the point bar along the inner bank of the downstream limb of the bend, two small headward eroding channels were present (Fig. 4A, G). Several headward eroding channels were also present along the right bank of the upstream limb of the bend (Fig. 4A). Just downstream of the bend apex, small mid-channel bars were present (Fig. 4A, arrowed).

4.1.2. Mid-chute cutoff

Later imagery (2007 onwards) shows that the westernmost headward eroding channel on the downstream limb developed into the chute channel, thereby connecting the upstream and downstream limbs (Fig. 4B, D). The mean width of the chute channel was 13 m in 2007, but underwent little

Journal Pre-proof

subsequent widening between 2007 and 2010 (Fig. 4B, C). The 2007 imagery shows that the sinuous embayment channel widened, especially in the downstream section (up to 6 m compared to 2 m in 2004), but did not develop into a chute channel (Fig. 4B, C). The other headward eroding channel on the downstream limb also connected with the upstream limb, and although it did not widen (Fig. 4B, C), the development of this channel and other erosional features increased surface roughness across the meander bend neck.

In the 2007 imagery, the in-channel bars were still present (Fig. 4B). By 2010, the mid-channel bar just downstream of the bend apex was less visible, with the flow path between the bar and the inner bank appearing to have infilled, and the upstream limb of the bend having narrowed slightly (Fig. 4C).

4.1.3. Post-chute cutoff

By 2013, all flow was being routed through the chute channel, indicating that the bend cutoff had been completed (Figs. 4D and 5B, C). Nevertheless, the chute channel (now the trunk channel) had irregular banklines, with width varying around an average of 13.4 m (Table 3), still narrower than the upstream and downstream limbs of the abandoned meander bend (average width of 27.4 m). Some headward eroding channels were still present across the neck of the bend. The mid-channel bar just downstream of the bend apex was no longer visible (Fig. 4D).

By 2016, the former chute channel had widened further (Fig. 4E) but was

Journal Pre-proof

still narrower than the upstream and downstream limbs of the abandoned meander bend (Table 3). Some headward eroding channels close to the former chute channel had widened up to 8.5 m (Figs. 4E and 5A), while those nearer the apex of the abandoned bend were narrower and had branching patterns (Fig. 5F). These trends continued through to the latter part of 2018. The 2018 imagery shows that the upstream part of the abandoned meander bend is now almost completely infilled, while at the apex and in the downstream limb of the bend, some standing water and/or damp sediments from the last rainy season were evident (Fig. 4F).

The high-resolution imagery shows that similar post-cutoff processes characterised CC1 and CC2 (Fig. 6). Channel banklines were narrower and more irregular in 2004 compared to the upstream and downstream limbs of the abandoned bends, which had been partially infilled (Fig. 6). The narrowest reach was less than 13 m wide along the former chute channel (now the trunk channel) at CC1 and less than 10 m wide along the chute channel at CC2, whereas the mean width of the former trunk channel was 21 m (Fig. 6). Later imagery (2007 onwards) shows that channel banklines along the former chute channels were more regular owing to erosional widening (Fig. 6).

4.2. Discharge regime and stream power controls

The catchment area upstream of the study reach is 2463 km^2. Bankfull discharge modelling using the Bjerklie (2007) method indicates that the

Journal Pre-proof

bankfull discharge is 54.8 $m^3 s^{-1}$ along the trunk channel, so discharge events exceeding 50 $m^3 s^{-1}$ will have potential for overbank flooding, either through crevasse channels or by bank overtopping. The discharge modelling results using the El-Hames (2012) method indicate that 34 flow events with peak discharge >50 $m^3 s^{-1}$ occurred during the 38 years between 1978 and 2016, with a maximum daily discharge of 345 $m^3 s^{-1}$ occurring on 24 December 2011 (Fig. 7A).

Although the study reach receives an average of one bankfull flow event each year, owing to the influence of ENSO dynamics, there is considerable interannual variability in the number of flood events and especially in peak flood magnitude. Figure 7B shows that cold (La Niña) phases of ENSO conditions tend to be associated with higher precipitation and thus more frequent, higher magnitude floods; events >50 $m^3 s^{-1}$ occurred four times in the rainy season of 2005 (maximum daily discharge of 196 $m^3 s^{-1}$), three times in 1981 and 2001, and twice in 1984 (maximum daily discharge of 277 $m^3 s^{-1}$), 1985, 1997, 2008, and 2013 (maximum daily discharge of 197 $m^3 s^{-1}$).

Discharge modelling by the El-Hames (2012) method of the annual maximum daily discharge for the period 1978-2016 derives a mean annual flood (Q_{af}) for the study reach of 98.85 $m^3 s^{-1}$. Based on dGPS surveys (Fig. 7C), the mean valley gradient through the study reach is 0.000232. At a local (short reach or individual bend) level, however, bankfull discharge and local gradient vary slightly, particularly as meander bends develop. While the mean

Journal Pre-proof

valley gradient of the study reach is 0.000232, in the middle part of the reach where most of the chute cutoffs have occurred (Fig. 1C), the gradient is slightly higher at 0.00028 (Fig. 7C). For CC3, bankfull discharge modelling by the Bjerklie (2007) method indicates that in 2013 the chute channel bankfull discharge was 16.9 m^3/s and in 2016 was 31.2 m^3/s, whereas the trunk channel bankfull discharge remained higher at 54.8 m^3/s (Table 3). Specific stream power was also slightly higher in the upstream limb of the trunk channel bend than in the chute channel both in 2013 and 2016 (Table 3).

4.3. Chute cutoff and meander bend morphometry and sedimentology

At CC3, fieldwork in 2015 demonstrated that the chute cutoff process had not been fully completed, although the abandoned meander bend had been largely infilled, particularly along the upstream limb. The chute channel remained narrower than the former trunk channel around the abandoned bend (Fig. 4E and Table 3). The chute channel banklines were irregular in contrast with the smooth banklines of the former trunk channel (Figs. 4E, 5B-D). Deposition had occurred at the entrance of the abandoned meander bend, forming a gentle slope compared to the adjacent riverbanks (Fig. 5D). It is likely that the gentle slope helped to promote flooding onto the neck of the bend, as suggested by observations of strandlines of fine organic litter aligned along the bend that likely could be attributed to the last bankfull event (Fig. 5D). Wide and shallow (less than 0.1 m deep) channels were present across the

Journal Pre-proof

neck of the bend, locally forming a branching pattern and connecting to the downstream limb of the abandoned bend (Fig. 5E, H). In addition, along the upstream limb of the now largely infilled abandoned bend, new headward eroding channels had formed on the right bank and had extended downstream across the bend (Figs. 4E and 5A, F). At a distance of ~155 m around the abandoned bend, the remaining depression was less than 0.15 m deep. In the downstream part of the abandoned bend, the depression was even shallower and was drained by a narrow gully.

Grain size analyses reveal that sediment (point bar deposits) along the present channel is composed mainly of silt and fine sand with a mean D_{50} of 118 μm, while floodplain sediment is dominantly clay and silt with a mean D_{50} of 33 μm. Channel fills in the abandoned bend at CC3 are also dominated by clay and silt (D_{50} <80 μm - Fig. 8). Trenches at the upstream end of the abandoned bend (T1 and T2; see the green dots in Fig. 5A for sampling locations) reveal that beneath the ~1 m thick channel fill, there is a cemented layer overlying green lacustrine mud at shallow depth. The channel fill is characterized by a fining-upward succession, consistent with observations of plug bar sedimentology made elsewhere (Constantine et al., 2010b). These trench samples also show that any coarser grain size fractions (i.e., fine sand) tend to decrease with distance around the abandoned bend.

At the downstream end of the abandoned meander bend, sediment is dominated by clay and silt (mean D_{50} ~20 μm) along with black organic mud,

Journal Pre-proof

which agrees with lateral accretion sediment exposed along the chute channel margins (T3 and T4 in Fig. 5A).

According to mapping of the changing orientation of scroll-bar sequences on high-resolution satellite imagery (Fig. 4G, H), the bend developed during two main periods of lateral accretion. The CC3 chute channel cuts through the two scroll-bar sequences, providing excellent exposure of the laterally accreted terrain that comprises this part of the floodplain (Fig. 9). Planar cross-bedding is the most prominent sedimentary structure, with apparent dips of 8° evident (Fig. 9). At the boundary between the two scroll-bar sequences, three small depressions with a width of up to ~1 m and depth of 0.2 m are filled with horizontally bedded, fine sediment (Fig. 9).

4.4. Interpretation

Our findings show that chute cutoffs are a prominent part of channel planform dynamics in the study reach of the Río Colorado (Figs. 1C and 2), with many developing rapidly on timescales of years to a few decades (Figs. 3-6). In this fine-grained, non-vegetated, ephemeral river, these findings prompt further consideration of the controls on overbank flow, chute cutoff development, and abandoned meander bend sedimentation.

4.4.1. Controls on overbank flow

Along the study reach of the Río Colorado, discharge modelling using the

Journal Pre-proof

Journal Pre-proof

El-Hames (2012) method demonstrates a high frequency of peak discharge >50 $m^3 s^{-1}$ (Fig. 7A), so bankfull channel cross-sectional area is regularly exceeded. In most years, near-bankfull or overbank flooding occurs at least once, but in some years overbank flooding occurs multiple times (e.g., 4 times in 2005). Around meander bends, additional factors promote overbank flow. First, the typically high divergence angles (average 98°) between the channel-belt axis and the entrance to the meander bend (Table 2) mean that during these peak discharge events, flow inertia promotes overbank flow along the tangential direction of the upstream limb of the meander bend. Second, as many meander bends elongate as a consequence of lateral migration, energy losses through the bend increase, and therefore flow efficiency decreases (e.g., Eaton and Church, 2004). For a given discharge around a bend of given width, this leads to a slowing of velocity and a corresponding increase in depth, also promoting local overbank flooding.

Adjacent to the upstream limb of meander bends, overbank floodwaters spread across the meander neck, commonly spilling back into the downstream limb of the meander bend. During falling stage, the increase in slope on the riverbank at the point of re-entry means that erosional channels are commonly initiated (cf. Donselaar et al., 2013) (Fig. 4). In the area of CC3, for instance, the alignment (102°) of the embayment channel and other headward eroding channels on the meander neck is almost the same as the tangential direction (101°) of the apex of the upstream bend (Fig. 4). Most of these headward

Journal Pre-proof

eroding channels developed along the centre of the channel axis, owing to the fact that overbank flow is likely greater around the upstream limb of the bend, with fewer headward eroding channels forming farther around the bend where overbank flow is probably less prominent (Fig. 4).

4.4.2. Controls on chute cutoff development

The satellite imagery shows that once initiated, some headward eroding channels develop rapidly during subsequent overbank flow events (Fig. 4). Although the rate of widening and deepening is dependent on the sequence of overbank flows experienced, several factors promote chute cutoff development. First, as noted above, the high divergence angles between the channel-belt axis and the upstream limb of the meander bend (Table 2) indicate that once formed, chute channels are more closely aligned with the general direction of flow along the channel-belt axis. Second, measurements indicate that abandoning or abandoned meander bend lengths are typically 4 times greater than chute channel lengths (Table 2), demonstrating the considerable gradient advantage of the chutes (cf. Grenfell et al., 2012) and the reduced total roughness of a shorter and straighter channel. Third, as also noted above, declining flow efficiency around the elongated meander bend contributes to a slowing of velocity, locally increasing depth for a given discharge and width, and promoting local overbank flooding. Slowing of velocity, however, also promotes sediment deposition at the bend entrance (see Section 4.3 and below)

Journal Pre-proof

Journal Pre-proof

and over time this tends to lead to a decrease in depth, further encouraging flow diversion to the chute channel.

4.4.3. Controls on meander bend sedimentation

The development of erosional features (embayments, headward eroding and chute channels) around abandoning meander bends generates sediment, some of which is deposited in the downstream limb of the meander bend. This interpretation is supported by the similar grain size distributions of sediment from channel fills in the downstream limb and from the laterally accreted terrain at CC3 (Figs. 8 and 9). In the early stages of cutoff development, water still flows around the abandoning bend but this downstream deposition contributes further to a decrease in flow velocity in the middle and upstream limb of the meander bend.

As a chute channel deepens and widens, it draws an increasing proportion of flow away from the abandoning meander bend. This also contributes to a decrease in flow velocity around the meander bend, further promoting deposition, especially in the upstream limb but also more widely around the bend. The disappearance of some channel bars at CC3 between 2007 and 2010 indicates that deposition occurred around the meander bend (Fig. 4B, C), even in the early stages of chute cutoff development.

4. Discussion

Journal Pre-proof

Journal Pre-proof

Some researchers consider chute channels to be keystone geomorphic features in the understanding of channel planform dynamics (e.g., Kleinhans and van den Berg, 2011; Grenfell et al., 2012). The findings from the lower Río Colorado are thus valuable because they provide new insights into the suite of factors that influence overbank flow, chute cutoff development, and meander bend sedimentation in a fine-grained, non-vegetated, ephemeral river. These insights provide scope for comparing the controls and importance of chute cutoffs in this river with other meandering river systems, both in dryland and more humid settings.

5.1. Climatic and non-climatic controls on cutoff development

Overbank flow has been regarded as one of major controls on the development of chute channels. Preferred pathways of overbank flow leading to chute channel development have commonly been attributed to the formation of a natural dam by woody debris or ice jams (e.g., Keller and Swanson, 1979; Gay et al., 1998; Thompson, 2003), or to shoaling of bedload sheets or unit bars (Peakall et al., 2007). Water is diverted from the upstream limb of a meander bend, flows across the meander bend neck, and rejoins the downstream limb of the bend. The plunging water on the downstream limb can initiate headward eroding channels, which may propagate upstream and cut through the meander neck to form chute channels. In the lower Río Colorado study area, however, the climatic and vegetative conditions means

Journal Pre-proof

that ice jams and large woody debris are not evident (Donselaar et al., 2013; Li et al., 2014a). As noted above, the characteristics of the study reach — including regular flood events in shallow channels (typically <1 m) and the high divergence angles between the channel-belt axis and upstream limb of many meander bends — appear to be sufficient conditions for chute initiation without damming effects. Furthermore, once formed, the high gradient advantage of the chute channel and sedimentation around the abandoning meander bend also contribute markedly to overbank flooding.

A critical question that arises, however, is how can such high-amplitude meander bends form in a low energy, fine-grained, non-vegetated setting? Given the low gradient (on average 0.000232 m/m) in the study reach and the relatively cohesive bed and bank sediments (dominantly silt and clay, locally with salt cementation), satellite imagery (Fig. 3) shows that many reaches have remained relatively stable, except for some meander bends that have migrated at rates of ~1m/yr or more. This bend migration accounts for much of the net erosion that occurred between 2004 and 2016 in the study reach (Fig. 10). The lower Río Colorado is dominated by rapid-rise flood events that have been shown to be a significant control on channel morphology and cascades of wider channel-floodplain changes (Li et al., 2014a,b, 2018, 2019). Discharge modelling results show that between 2004 and 2016 only 16 days have experienced discharges >10 $m^3 s^{-1}$, but that many of these events have been >50 $m^3 s^{-1}$. Significant net erosion occurred between 2004 and 2007,

Journal Pre-proof

and was probably related to four peak discharge events >50 $m^3 s^{-1}$ that occurred in 2005 (Fig. 10). Substantial erosion occurred at CC1 and CC2 as evidenced by the irregularity of channel banklines, and was only partially offset by sedimentation around the former meander bends. For CC1, the total area of net erosion was 4253 m^2 between 2004 and 2007, and for CC2 was 1536 m^2 between 2004 and 2007. Similiarly, three peak discharge events >50 $m^3 s^{-1}$, including the largest flood on record (346 $m^3 s^{-1}$), occurred between 2011 and 2013 (Fig. 10). For CC1 and CC2, the total area of net erosion between 2010 and 2013 was 712 m^2 and 750 m^2 respectively, and for CC3, there was also moderate net erosion and completion of the cutoff (Figs. 4 and 10).

A comparison between our discharge modelling results and the multivariate ENSO MEI index (Fig. 7A, B) reveals that many peak discharge events are closely related to La Niña events. These findings strongly suggest the possibility that along the Río Colorado, short-term (yearly to decadal) bend dynamics are strongly conditioned by episodic climatic forcing. This situation may lead to short-lived phases of enhanced bend migration and clusters of cutoff (cf. Hooke, 2008), punctuating a longer term (multidecadal to centennial) pattern of slow lateral migration and periodic avulsion. Avulsion dynamics add complications to rates and patterns of bend development; the Landsat imagery shows that the downstream part of the present trunk channel in the study reach was active in 1975 (Fig. 2, reach B), was partially abandoned owing to upstream avulsion that occurred between 1975 and 1996 (Fig. 2, reach A to

Journal Pre-proof

reaches C and D), and was reactivated by 2001 as a result of another avulsion (Fig. 2, reach D back to reach B). Such reoccupation of previously abandoned, remnant meanders may increase bend development rates (e.g., faster lateral migration, more frequent cutoff events), because bend development is rekindled from a starting point of already sinuous, rather than newer, straighter channels.

Similar cyclicities of meander planform dynamics (including chute cutoff initiation) and floodplain activity have been observed in other rivers, both in humid (Brewer and Lewin, 1998; Hooke, 2008) and tropical regions (Aalto et al., 2003). For instance, on the River Severn at Llandinam, Wales, planform cyclicity through the meandering to moderately braided transition has also been linked to climatic cycles (Brewer and Lewin, 1998). In the Beni River, Bolivia, distal floodplain sedimentation is driven by large, rapid-rise floods that occur episodically in association with La Niña (Aalto et al., 2003). In the lower Río Colorado, planform cyclicity in terms of the frequency of chute initiation and cutoff development is strongly influenced by episodic La Niña flood peaks that provide the energy needed to exceed the cohesion of bed, bank and floodplain surfaces (in the lowermost reaches, including the lacustrine muds over which the channel belt is prograding), thereby enabling more rapid meander bend lengthening, and more frequent chute channel initiation and bend cutoff events. By contrast, in intervals with normal or low frequency flood peak activity, cohesion is overcome less regularly and for shorter periods of time, resulting in

Journal Pre-proof

slower rates of bend development and less frequent cutoff events. The allogenic (climate) drivers of meander dynamics observed in these rivers contrast with some field and modelling studies that have tended to focus on clusters of cutoffs that result from autogenic drivers, namely those related to intrinsic meander bend dynamics (e.g., Stølum, 1996, 1998; Hooke, 2007), but correspond with Hooke's (2008) field observations that the nature and timing of floods largely determine the timing of cutoff. The 1D meander migration models that have been used to investigate autogenic behavior (e.g., self-organized criticality) generally apply neck cutoff rules. Neck cutoff results in larger increases in local channel gradient relative to chute cutoff, so the potential for these autogenic gradient-disturbances to cascade through the system and drive intrinsic spatio-temporal clustering of cutoff occurrence is greater than for chute cutoff (Camporeale et al., 2008).

Along the Río Colorado, sediment cohesion is sufficient to maintain an overall single-thread channel planform even in the absence of floodplain vegetation, but is not so cohesive as to result in planform ossification, a finding that is consistent with the flume observations of Peakall et al. (2007). The net result of slow rates of bend development, punctuated by clusters of chute cutoffs, is a river system that retains an overall low to moderate sinuosity (cf. Howard, 1996). The findings from the Río Colorado thus illustrate that floodplain vegetation is not a necessary condition for the maintenance of dynamic single-thread meandering (or the suppression of a sustained transition

Journal Pre-proof

to braiding) in fine-bed systems, as it may be in coarse-bed systems (e.g., Braudrick et al., 2009).

5.2. Comparing cutoff dynamics in ephemeral and perennial rivers

In drylands, meandering rivers traditionally have been considered to be limited in extent compared to other planform types (Graf, 1988; Tooth, 2000, 2013). Most previously documented examples of dryland meandering rivers have been from settings where perennial rivers flow from humid regions into the dryland (e.g., Gilvear et al., 2000; Tooth and McCarthy, 2004; Pietsch and Nanson, 2011; Hesse et al., 2018), or where seasonal rainfall or snowmelt supports perennial or intermittent flow (e.g., Marren et al., 2006; Grenfell et al., 2012; Keen-Zebert et al., 2013; Larkin et al., 2017).

In recent years, however, greater focus has been directed towards a more complete documentation of the distribution, forms, dynamics and sedimentology of ephemeral meandering rivers in drylands (Billi et al. 2018; Ielpi, 2018; Ielpi and Lapôtre, 2019; Santos et al., 2019). This work has enabled the use of sparsely- or non-vegetated dryland river systems as actualistic models for improved interpretations of Earth's pre-vegetation rock record and as analogues for meandering fluvial forms on vegetation-free planetary bodies. Using satellite imagery, preliminary global datasets on dryland meandering rivers have been assembled (Billi et al., 2018; Santos et al., 2019). These datasets tend to include a mix of dryland meandering types with

Journal Pre-proof

diverse vegetation assemblages (fully, sparsely or non-vegetated), and varying degrees of lateral activity from actively meandering through to essentially static ('stable sinuous' planforms - cf. Tooth and McCarthy, 2004). In the absence of flow data, many of these rivers are assumed to have ephemeral flow regimes, but it is possible that some may have intermittent or perennial flow. Regardless of these limitations, the datasets have documented the wider existence of meandering rivers in drylands than has been appreciated hitherto, but there remains a need for an improved mechanistic understanding of ephemeral meander bend dynamics, as well as greater documentation of the sedimentological implications of bend development and abandonment, whether by chute or neck cutoff. Notable exceptions exist; for example, Ielpi (2018) studied the ephemeral, non-vegetated, lower Amargosa River in Death Valley, California, USA, and documented that over two decades or more, some sinuous channels <2 m deep and <35 m wide migrated laterally at rates <1.5 m/yr while others displayed virtually no planform change. The migration of larger channels (width/depth ratios ~4) generates scroll bars and inclined sedimentary packages but the migration of the more widespread, smaller meanders (width/depth ratios ~40) only generates sub-tabular sets. Along the lower Amargosa River, although some meander bends display evidence of past cutoff events and present-day active chute channels, episodes of neck or chute cutoff have not been directly observed (Ielpi, 2018).

In the light of these studies, the findings from the lower Río Colorado

Journal Pre-proof

provide valuable additional insights into the controls, forms and processes of ephemeral meanders. First, in this non-vegetated setting, significant planform adjustments (avulsion, bend migration, cutoff development) are occurring on a timescale of years to decades, contrasting with some other dryland settings where many meander bends are essentially forms inherited from prior, wetter climatic intervals, and development only occurs very slowly under present-day hydroclimatic regimes (e.g., Tooth, 1997; Nanson and Tooth, 1999; Tooth and McCarthy, 2004; Larkin, 2019). Along the active bends of the Río Colorado, for instance, time series of high-resolution satellite imagery and field investigations can help document processes of cutoff development, as well as the sedimentological consequences of bend abandonment, in ways that are not possible in many other dryland settings. Second, the apparent dominance of chute cutoff along the Río Colorado contrasts with some other dryland meandering rivers where neck cutoff appears to be more dominant (e.g., Tooth et al., 2002; Keen-Zebert et al., 2013; Larkin et al., 2017) or where there is a greater mix of neck and chute cutoff (e.g. Z. Li et al., 2017). Third, and moving beyond just drylands, the study of bend dynamics along the Río Colorado complements flume-based studies of chute cutoff development in non-vegetated, cohesive sediments (Smith, 1998; Peakall et al., 2007; Van Dijk et al., 2013) and field studies of meander dynamics in cohesive sediments in non-dryland fluvial and tidal settings (e.g., Rhoads and Miller, 1991; Kleinhans et al., 2009). Our findings also contribute to a better understanding of low

Journal Pre-proof

energy, fine-grained, contemporary meandering rivers in general (e.g., Page et al., 2003; Brooks, 2003; Marren et al., 2006), complementing the more numerous studies of higher energy, sand- and gravel-bed meanders.

5. Conclusions

The low energy, fine-grained Río Colorado provides a rare example of an ephemeral river that meanders in the absence of vegetative influences, with active bend development occurring on yearly to decadal timescales. Satellite imagery and field observations have been used to investigate chute cutoff-driven meander bend abandonment and sedimentation along a 25 km long study reach. Three recent chute cutoffs have been investigated in detail; for one of these bends, high-resolution imagery reveals the details of pre-, mid- and post-chute cutoff processes. Results indicate that for any given bend, an increase in bend amplitude and a high divergence angle between the channel-belt axis and the upstream limb of the meander bend leads to declining flow efficiency, thereby promoting overbank flooding as well as deposition within the upstream limb of the bend. Overbank flooding promotes the development of headward eroding channels, some of which may rapidly develop into shallow chute channels. Additionally, sediment yielded by headward erosion and by overbank flow tends to be deposited in the downstream limb of abandoning bends due to increasing roughness created by chute channels and other erosional features across the neck of the meander

Journal Pre-proof

bend. Deposition tends to further reduce the sediment transport capacity of the bend, leading to deposition in its upstream limb. During subsequent floods, deepening and widening of the chute channel and infilling of the meander bend continues. In this setting, potential specific stream power and bed and bank cohesion are sufficient to maintain slow but active bend migration, punctuated episodically by La Niña-driven phases of enhanced flooding and chute cutoff, such that a low to moderate sinuosity single-thread planform is maintained in the long term.

The Río Colorado is unusual but not unique, and similar morphodynamics may characterize other ephemeral meandering rivers worldwide, especially those that terminate on the margins of salt lakes (Li et al., 2019). Along with further studies of these other rivers, the findings from the Río Colorado will contribute to a more comprehensive understanding of contemporary meandering river dynamics, and may also help to improve interpretations of Earth's pre-vegetation rivers and meandering fluvial forms on other planetary bodies (cf. Ielpi, 2018; Santos et al., 2019). Hence, a key agenda for future research should be to initiate additional detailed field studies of ephemeral meandering rivers across a wider range of Earth's diverse drylands, which are characterised by varied combinations of climatic, physiographic, tectonic, vegetative and edaphic conditions. This will enhance preliminary global datasets of dryland meandering rivers by enabling assessment of the relative importance of neck versus chute cutoff, as well as better constraining rates and

Journal Pre-proof

timescales of cutoff development.

Declaration of interests

The authors declare that they have no known competing financial interests or personal relationships that could have appeared to influence the work reported in this paper.

The authors declare the following financial interests/personal relationships which may be considered as potential competing interests:

Authors: Jiaguang Li, Michael C. Grenfell, Hao Wei, Stephen Tooth, Sophea Ngiem

Acknowledgements

This research was supported by the National Natural Science Foundation of China (No. 41602121, No. 41972114), the Open Fund (PLC20180502) of State Key Laboratory of Oil and Gas Reservoir Geology and Exploration (Chengdu University of Technology, Chengdu, China), and the Fundamental Research Funds for the Central Universities, China University of Geosciences (Wuhan) (No. CUG150616) and Open Fund (TPR-2017-01) of Key Laboratory (Ministry of Education) of Tectonics and Petroleum Resources (China University of Geosciences, Wuhan, China). JL is grateful for the financial support by China Scholarship Council (CSC) as visiting scholar at Aberystwyth University. JL thanks colleagues Oswaldo Eduardo Ramos Ramos, Rafael Cortez, and students Edson Wilder Ramos Mendoza, Wilhelm Alex Mendizabal Cuevas, Samir Nikolar Pacheco, Erick Marcelo Cabero Caballero, and Julian Franz Cortez Garvizu from Universidad Mayor de San Andrés for the fieldwork arrangements and assistance in Salar de Uyuni, Bolivia. Editor Scott Lecce and reviewers Paolo Billi and Alessandro Ielpi are thanked for their constructive comments that helped to improve the final submission.

Journal Pre-proof

Journal Pre-proof

References

Aalto, R., Maurice-bourgoin, L., Dunne, T., 2003. Episodic sediment accumulation on Amazonian flood plains influenced by El Nino/Southern Oscillation. Nature 425, 493–497.

Baucom, P.C., Rigsby, C.A., 1999. Climate and lake-level history of the northern Altiplano, Bolivia, as recorded in Holocene sediments of the Rio Desaguadero. J. Sediment. Res. 69, 597–611.

Billi, P., Demissie, B., Nyssen, J., Moges, G., Fazzini, M., 2018. Meander hydromorphology of ephemeral streams: Similarities and differences with perennial rivers. Geomorphology 319, 35–46.

Bills, B.G., de Silva, S.L., Currey, D.R., Emenger, R.S., Lillquist, K.D., Donnellan, A., Worden, B., 1994. Hydro-isostatic deflection and tectonic tilting in the central Andes: Initial results of a GPS survey of Lake Minchin shorelines. Geophys. Res. Lett. 21, 293–296.

Bjerklie, D.M., 2007. Estimating the bankfull velocity and discharge for rivers using remotely sensed river morphology information. J. Hydrol. 341, 144–155.

Braudrick, C.A., Dietrich, W.E., Leverich, G.T., Sklar, L.S., 2009. Experimental evidence for the conditions necessary to sustain meandering in coarse-bedded rivers. Proc. Natl. Acad. Sci. 106, 16936–16941.

Journal Pre-proof

Journal Pre-proof

Brewer, P.A., Lewin, J., 1998. Planform cyclicity in an unstable reach: Complex fluvial response to environmental change. Earth Surf. Process. Landforms 23, 989–1008.

Bridge, J.S., 2003. Rivers and Floodplains: Forms, Processes, and Sedimentary Record. Blackwell Science Ltd., Oxford, UK.

Bridge, J.S., Smith, N.D., Trent, F., Gabel, S.L., Bernstein, P., 1986. Sedimentology and morphology of a low-sinuosity river: Calamus River, Nebraska Sand Hills. Sedimentology 33, 851–870.

Brooks, G.R., 2003. Holocene lateral channel migration and incision of the Red River, Manitoba, Canada. Geomorphology 54, 197–215.

Constantine, J.A., Dunne, T., 2008. Meander cutoff and the controls on the production of oxbow lakes. Geology 36, 23–26.

Constantine, J.A., Dunne, T., Piégay, H., Mathias Kondolf, G., 2010a. Controls on the alluviation of oxbow lakes by bed-material load along the Sacramento river, California. Sedimentology 57, 389–407.

Constantine, J.A., McLean, S.R., Dunne, T., 2010b. A mechanism of chute cutoff along large meandering rivers with uniform floodplain topography. Bull. Geol. Soc. Am. 122, 855–869.

Donselaar, M.E., Gozalo, M.C.C., Moyano, S., 2013. Avulsion processes at the terminus of low-gradient semi-arid fl uvial systems : Lessons from the Río Colorado , Altiplano endorheic basin , Bolivia. Sediment. Geol. 283, 1–14.

Journal Pre-proof

Journal Pre-proof

Eaton, B.C., Church, M., 2004. A graded stream response relation for bed load–dominated streams Brett. J. Geophys. Res. 109, 1–18.

El-Hames, A.S., 2012. An empirical method for peak discharge prediction in ungauged arid and semi-arid region catchments based on morphological parameters and SCS curve number. J. Hydrol. 456–457, 94–100.

Elger, K., Oncken, O., Glodny, J., 2005. Plateau-style accumulation of deformation: Southern Altiplano. Tectonics 24. TC4020.

Fisk, H.N., 1944. Geological Investigation of the Alluvial Valley of the Lower Mississippi River. US Army Corps Eng. Mississippi River Comm. Vicksburg, MS.

Fisk, H.N., 1947. Fine-Grained Alluvial Deposits and their Effects on Mississippi River Activity. US Army Corps Eng. Mississippi River Comm. Vicksburg, MS.

Gagliano, S.M., Howard, P.G., 1984. The neck cutoff oxbow lake cycle along the Lower Mississippi River, in: Elliot, C.M. (Ed.), River Meandering. American Society of Civil Engineers, New Orleans, LA, pp. 147–158.

Gay, G.R., Gay, H.H., Gay, W.H., Martinson, H.A., Meade, R.H., Moody, J.A., 1998. Evolution of cutoffs across meander necks in Powder River, Montana, USA. Earth Surf. Process. Landforms 23, 651–662.

Ghinassi, M., Colombera, L., Mountney, N.P., Reesink, A.J.H., 2018. Sedimentology of meandering river deposits: advances and challenges, in: Ghinassi, M., Colombera, L., Mountney, N.P. and Reesink A.J.H. (Ed.), Fluvial Meanders and Their Sedimentary Products in the Rock Record. International Association of Sedimentologists Special Pulication 48, 1–14.

Journal Pre-proof

Journal Pre-proof

Gilvear, D., Winterbottom, S., Sichingabula, H., 2000. Character of channel planform change and meander development Luangwa River, Zambia. Earth Surface Processes and Landforms 436, 421–436.

Graf, W.L., 1988. Fluvial Processes in Dryland Rivers. Springer-Verlag, New York.

Grenfell, M., Aalto, R., Nicholas, A., 2012. Chute channel dynamics in large, sand-bed meandering rivers. Earth Surf. Process. Landforms 37, 315–331.

Hesse, P.P., Williams, R., Ralph, T.J., Fryirs, K.A., Larkin, Z.T., Westaway, K.E., Farebrother, W., 2018. Palaeohydrology of lowland rivers in the Murray-Darling Basin, Australia. Quat. Sci. Rev. 200, 85–105.

Hooke, J.M., 1995. River channel adjustment to meander cutoffs on the River Bollin and River Dane, northwest England. Geomorphology 14, 235–253.

Hooke, J.M., 2004. Cutoffs galore!: Occurrence and causes of multiple cutoffs on a meandering river. Geomorphology 61, 225–238.

Hooke, J.M., 2008. Temporal variations in fluvial processes on an active meandering river over a 20-year period. Geomorphology 100, 3–13.

Horton, B.K., Decelles, P.G., 2001. Modern and ancient fluvial megafans in the foreland basin system of the central Andes, southern Bolivia: implications for drainage network evolution in fold-thrust belts. Basin Res. 13, 43–63.

Howard, A.D., 1996. Modelling channel evolution and floodplain morphology, in: Anderson, M.G., Walling, D.E., Bates, P.D. (Eds.), Floodplain Processes. John Wiley, Chichester, pp. 15–62.

Journal Pre-proof

Journal Pre-proof

Ielpi, A., 2018. Morphodynamics of meandering streams devoid of plant life: Amargosa River, Death Valley, California. GSA Bull. 131, 782–802.

Ielpi, A., Lapôtre, M.G.A., 2019. Barren meandering streams in the modern Toiyabe basin of Nevada, U.S.A., and their relevance to the study of the pre-vegetation rock record. J. Sediment. Res. 89, 399–415.

Jackson II, R.G., 1976. Depositional model of point bars in the Lower Wabash River. J. Sediment. Petrol. 46, 579–594.

Keen-Zebert, A., Tooth, S., Rodnight, H., Duller, G.A.T., Roberts, H.M., Grenfell, M., 2013. Late Quaternary floodplain reworking and the preservation of alluvial sedimentary archives in unconfined and confined river valleys in the eastern interior of South Africa. Geomorphology 185, 54–66.

Keller, E.A., Swanson, F.J., 1979. Effects of large organic material on channel form and fluvial processes. Earth Surf. Process. 4, 361–380.

Kleinhans, M.G., Schuurman, F., Bakx, W., Markies, H., 2009. Meandering channel dynamics in highly cohesive sediment on an intertidal mud flat in the Westerschelde estuary, the Netherlands. Geomorphology 105, 261–276.

Kleinhans, M.G., van den Berg, J.H., 2011. River channel and bar patterns explained and predicted by an empirical and a physics-based method. Earth Surf. Process. Landforms 36, 721–738.

Konert, M., Vandenberghe, J., 1997. Comparison of laser grain size analysis with pipette and sieve analysis: a solution for the underestimation of the clay fraction. Sedimentology 44, 523–535.

Journal Pre-proof

Journal Pre-proof

Larkin, Z.T., 2019. Dryland rivers and hydroclimatic change: past, present and future. Unpublished PhD thesis, Macquarie University, Australia.

Larkin, Z.T., Tooth, S., Ralph, T.J., Duller, G.A.T., McCarthy, T., Keen-Zebert, A., Humphries, M.S., 2017. Timescales, mechanisms, and controls of incisional avulsions in floodplain wetlands: Insights from the Tshwane River, semiarid South Africa. Geomorphology 283, 158–172.

Lenters, J.D., Cook, K.H., 1999. Summertime precipitation variability over South America: Role of the large-scale circulation. Mon. Weather Rev. 127, 409–431.

Lewis, G.W., Lewin, J., 1983. Alluvial cutoffs in Wales and the Borderlands. International Association of Sedimentologists Special Pulication 6, 145–154.

Li, J., 2014. Terminal fluvial systems in a semi-arid endorheic basin, Salar de Uyuni (Bolivia). Uitgeverij BOX Press, 's-Hertogenbosch, The Netherlands.

Li, J., Bristow, C.S., 2015. Crevasse splay morphodynamics in a dryland river terminus: Río Colorado in Salar de Uyuni Bolivia. Quat. Int. 377, 71–82.

Li, J., Bristow, C.S., Luthi, S.M., Donselaar, M.E., 2015b. Dryland anabranching river morphodynamics: Río Capilla, Salar de Uyuni, Bolivia. Geomorphology 250, 282–297.

Li, J., Donselaar, M.E., Hosseini Aria, S.E., Koenders, R., Oyen, A.M., 2014a. Landsat imagery-based visualization of the geomorphological development at the terminus of a dryland river system. Quat. Int. 352, 100–110.

Li, J., Luthi, S.M., Donselaar, M.E., Weltje, G.J., Prins, M.A., Bloemsma, M.R., 2015a. An ephemeral meandering river system: Sediment dispersal processes in the

Journal Pre-proof

Journal Pre-proof

Río Colorado, Southern Altiplano Plateau, Bolivia. Zeitschrift für Geomorphol. 59, 301–317.

Li, J., Menenti, M., Mousivand, A., Luthi, S.M., 2014b. Non-vegetated playa morphodynamics using multi-temporal landsat imagery in a semi-arid endorheic basin: Salar de Uyuni, Bolivia. Remote Sens. 6, 10131–10151.

Li, J., Tooth, S., Yao, G., 2019. Cascades of sub-decadal, channel-floodplain changes in low-gradient, non-vegetated reaches near a dryland river terminus: Salar de Uyuni, Bolivia. Earth Surf. Process. Landforms 44, 490–506.

Li, J., Yang, X., Maffei, C., Tooth, S., Yao, G., 2018. Applying independent component analysis on Sentinel-2 imagery to characterize geomorphological responses to an extreme flood event near the non-vegetated Río Colorado terminus, Salar de Uyuni, Bolivia. Remote Sens. 10, 725.

Li, Z., Yu, G.A., Brierley, G.J., Wang, Z., Jia, Y., 2017. Migration and cutoff of meanders in the hyperarid environment of the middle Tarim River, northwestern China. Geomorphology 276, 116–124.

Marren, P.M., McCarthy, T.S., Tooth, S., Brandt, D., Stacey, G.G., Leong, A., Spottiswoode, B., 2006. A comparison of mud- and sand-dominated meanders in a downstream coarsening reach of the mixed bedrock-alluvial Klip River, eastern Free State, South Africa. Sediment. Geol. 190, 213–226.

Marshall, L.G., Iii, C.C.S., Lavenu, A., Hoffstetter, R., Curtis, G.H., 1992. Geochronology of the mammal-bearing late Cenozoic on the northern Altiplano, Bolivia. J. South Am. Earth Sci. 5, 1–19.

Journal Pre-proof

Journal Pre-proof

Miall, A.D., 1996. The geology of fluvial deposits. Springer, New York.

Nanson, G.C., Tooth, S., 1999. Arid-zone rivers as indicators of climate change, in: Singhvi, A.K., Derbyshire, E. (Eds.), Paleoenvironmental Reconstruction in Arid Lands. A.A. Balkema, Rotterdam, pp. 175–216.

Page, K.J., Nanson, G.C. and Frazier, P.S., 2003. Floodplain formation and sediment stratigraphy resulting from oblique accretion on the Murrumbidgee River, Australia. J. Sediment. Res. 73, 5–14.

Peakall, J., Ashworth, P.J., Best, J.L., 2007. Meander-bend evolution, alluvial architecture, and the role of cohesion in sinuous river channels: A flume study. J. Sediment. Res. 77, 197–212.

Pietsch, T.J., Nanson, G.C., 2011. Bankfull hydraulic geometry; the role of in-channel vegetation and downstream declining discharges in the anabranching and distributary channels of the Gwydir distributive fluvial system, southeastern Australia. Geomorphology 129, 152–165.

Rhoads, B.L., Miller, M. V., 1991. Impact of flow variability on the morphology of a low-energy meandering river. Earth Surf. Process. Landforms 16, 357–367.

Rigsby, C.A., Bradbury, J.P., Baker, P.A., Rollins, S.M., Warren, M.R., 2005. Late Quaternary palaeolakes, rivers, and wetlands on the Bolivian Altiplano and their palaeoclimatic implications. J. Quat. Sci. 20, 671–691.

Santos, M.G.M., Hartley, A.J., Mountney, N.P., Peakall, J., Owen, A., Merino, E.R., Assine, M.L., 2019. Meandering rivers in modern desert basins: Implications for channel planform controls and prevegetation rivers. Sediment. Geol. 385, 1–14.

Journal Pre-proof

Journal Pre-proof

Schwenk, J., Foufoula-Georgiou, E., 2016. Meander cutoffs nonlocally accelerate upstream and downstream migration and channel widening. Geophys. Res. Lett. 43, 12,437-12,445.

Smith, C.E., 1998. Modeling high sinuosity meanders in a small flume. Geomorphology 25, 19–30.

Smith, D.G., Pearce, C.M., 2002. Ice jam-caused fluvial gullies and scour holes on northern river flood plains. Geomorphology 42, 85–95.

Stølum, H.-H., 1996. River meandering as a self-organization process. Science 271, 1710–1713.

Stølum, H.H., 1998. Planform geometry and dynamics of meandering rivers. Geol. Soc. Am. Bull. 110, 1485–1498.

Thompson, D.M., 2003. A geomorphic explanation for a meander cutoff following channel relocation of a coarse-bedded river. Environ. Manage. 31, 385–400.

Tooth, S., 1997. The Morphology, Dynamics and Late Quaternary Sedimentary History of Ephemeral Drainage Systems on the Northern Plains of Central Australia. Unpublished PhD thesis, University of Wollongong, Australia.

Tooth, S., 2000. Process, form and change in dry land rivers: a review of recent research. Earth-Science Rev., 51, 67–107.

Tooth, S., 2013. Dryland Fluvial Environments: Assessing Distinctiveness and Diversity from a Global Perspective. In: Shroder, J.F. (Ed.), Treatise on Geomorphology, Academic press, San Diego, 612–644.

Journal Pre-proof

Journal Pre-proof

Tooth, S., McCarthy, T.S., 2004. Controls on the transition from meandering to straight channels in the wetlands of the Okavango Delta, Botswana. Earth Surf. Process. Landforms 29, 1627–1649. doi:10.1002/esp.1117

Tooth, S., McCarthy, T.S., Brandt, D., Hancox, P.J., Morris, R., 2002. Geological controls on the formation of alluvial meanders and floodplain wetlands: The example of the Klip River, eastern Free State, South Africa. Earth Surf. Process. Landforms 27, 797–815.

van Dijk, W.M., Van De Lageweg, W.I., Kleinhans, M.G., 2012. Experimental meandering river with chute cutoffs. J. Geophys. Res. Earth Surf. 117, 1–18.

van Dijk, W.M., Van de Lageweg, W.I., Kleinhans, M.G., 2013. Formation of a cohesive floodplain in a dynamic experimental meandering river. Earth Surf. Process. Landforms 38, 1550–1565.

van Toorenenburg, K.A., Donselaar, M.E., Weltje, G.J., 2018. The life cycle of crevasse splays as a key mechanism in the aggradation of alluvial ridges and river avulsion. Earth Surf. Process. Landforms 43, 2409–2420.

Zinger, J.A., Rhoads, B.L., Best, J.L., 2011. Extreme sediment pulses generated by bend cutoffs along a large meandering river. Nat. Geosci. 4, 675–678.

Fig. 1 The Altiplano and the Río Colorado catchment: (A) location of the Altiplano in South America; (B) map of the Altiplano, highlighting the study reach of the Río Colorado (red box) near the southeastern margin of the Salar de Uyuni; (C) details of study reach,

Journal Pre-proof

showing the areas covered by some subsequent figures. The blue line indicates the current trunk channel (see Fig. 2) and the dashed line labelled S and N indicates the dGPS measurement path (see Fig. 7C).

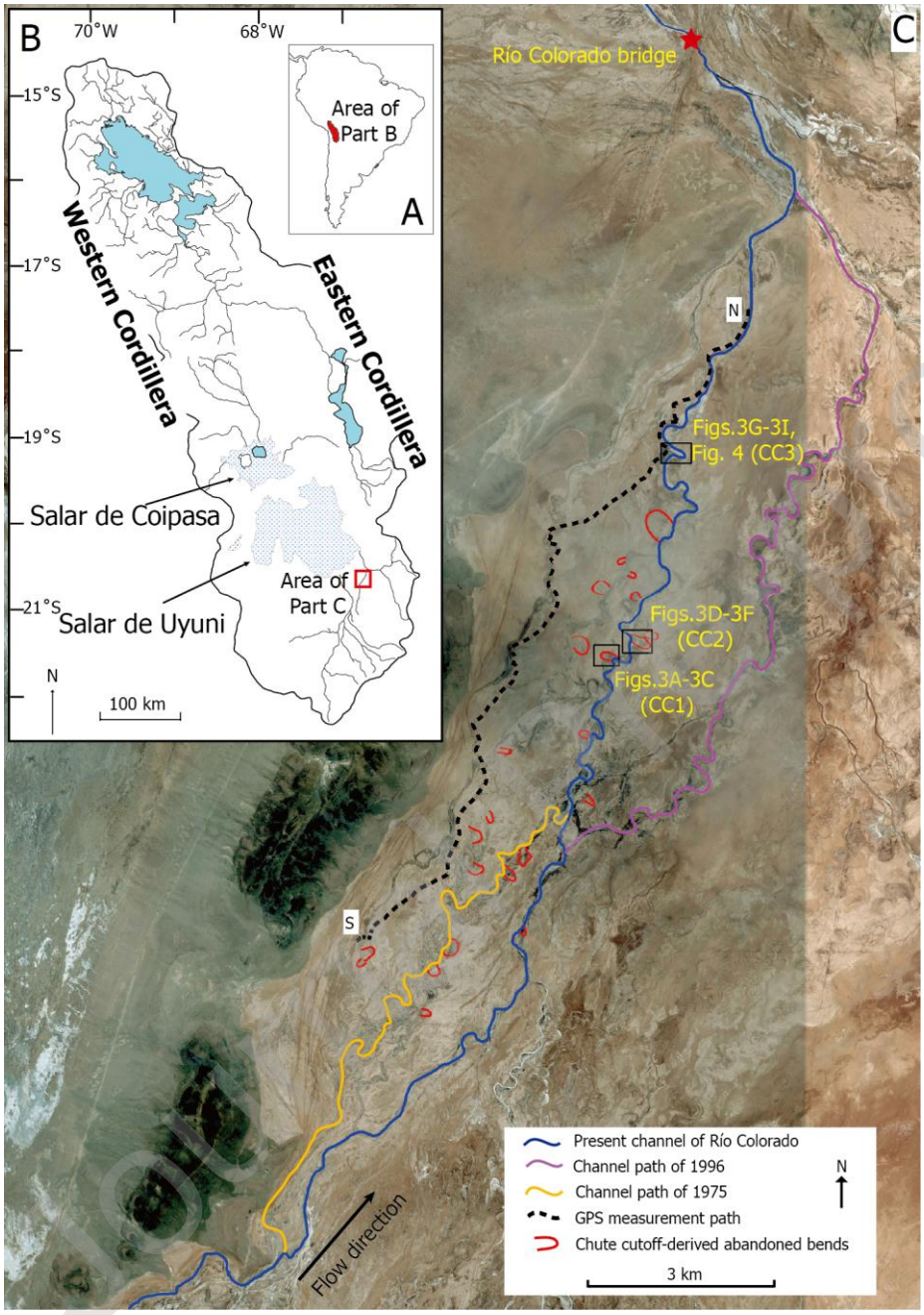

Fig. 2 Decadal-scale avulsion history in the study reach, reconstructed using Landsat imagery from March 1975 through November 2001.

Journal Pre-proof

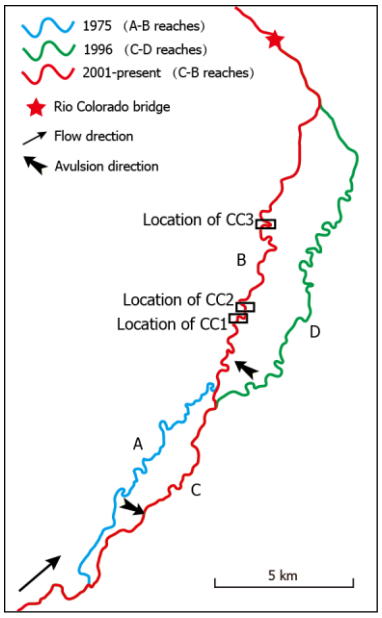

Fig. 3 Development of three chute cutoffs (indicated by red boxes) in the study reach, visualised using Landsat imagery (A-F) with a spatial resolution of 30 m and ASTER imagery (G-I) with a spatial resolution of 15 m: A-C) chute channel 1 (CC1); D-F) chute channel 2 (CC2); G-I) chute channel 3 (CC3).

Journal Pre-proof

Journal Pre-proof

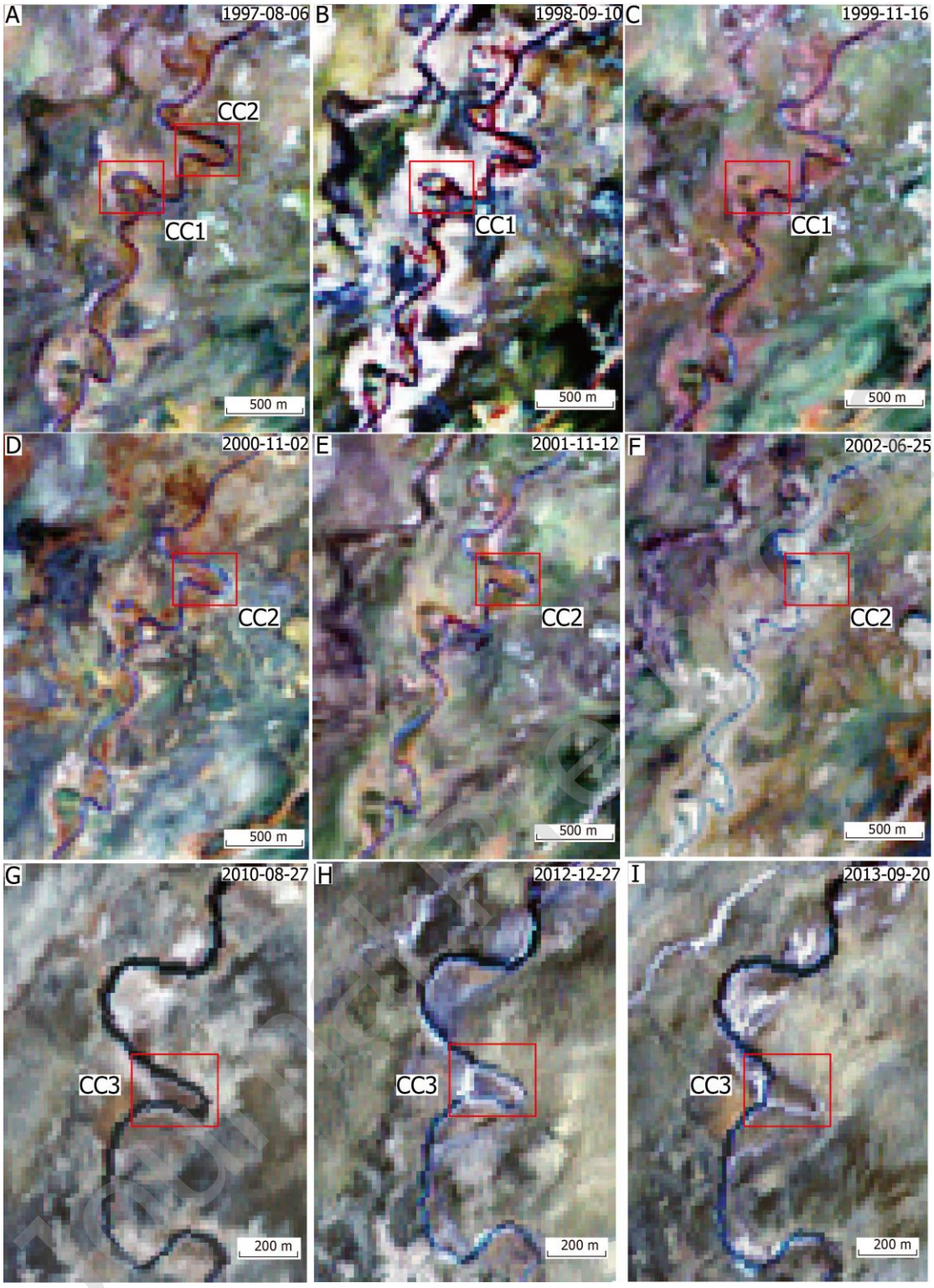

Fig. 4 (A-F) Development of chute cutoff 3, visualised using high-resolution (<0.65 m) satellite imagery from November 2004 through November 2018. To provide a common reference point, an arrow in A-F indicates channel bars in the apex of the meander; (G-H) interpretation sketches showing key geomorphological and sedimentological features and

Journal Pre-proof

the development of chute cutoff 3 (the sketch in G is based on image A while the sketch in H is based on image E).

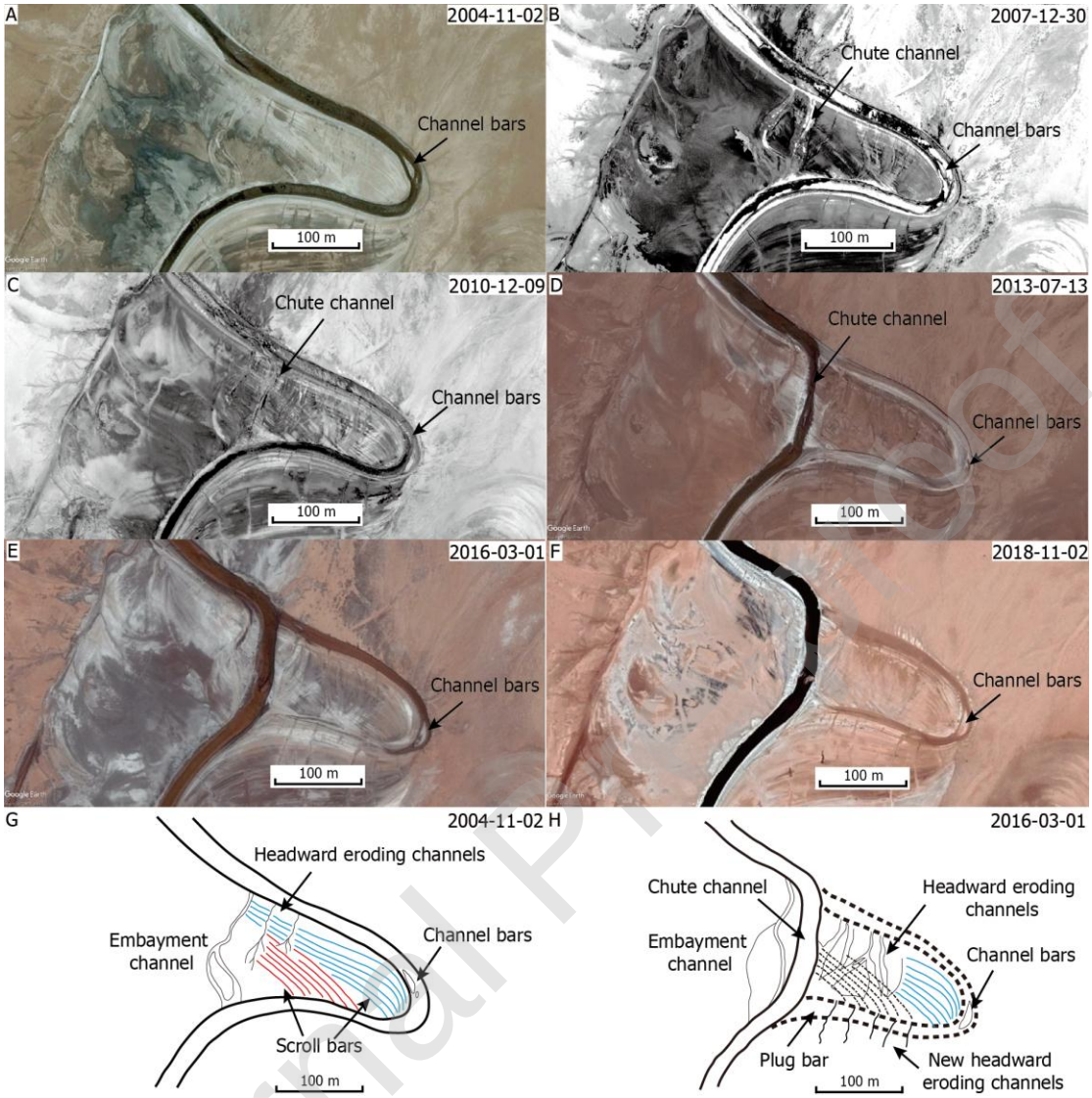

Fig. 5 Photographs of the geomorphological features in the vicinity of chute cutoff CC3 (in B-F, scales are for the foreground): (A) locations of trenches (T1-T4) and photographs for parts B-F and Fig. 9; (B) chute channel (view looking downstream) with the embayment channel on far left; (C) chute channel and trunk channel beds (view looking upstream); (D) gentle bed slope at the entry to the abandoned meander bend as well as organic debris (arrowed) left aligned on the uppermost part of the chute channel right bank during the last flood recession (view looking downstream along the chute channel); (E) headward

Journal Pre-proof

eroding channel (view looking downstream) adjacent to the chute channel; (F) bifurcation along a headward eroding channel on the meander bend neck (view looking downstream).

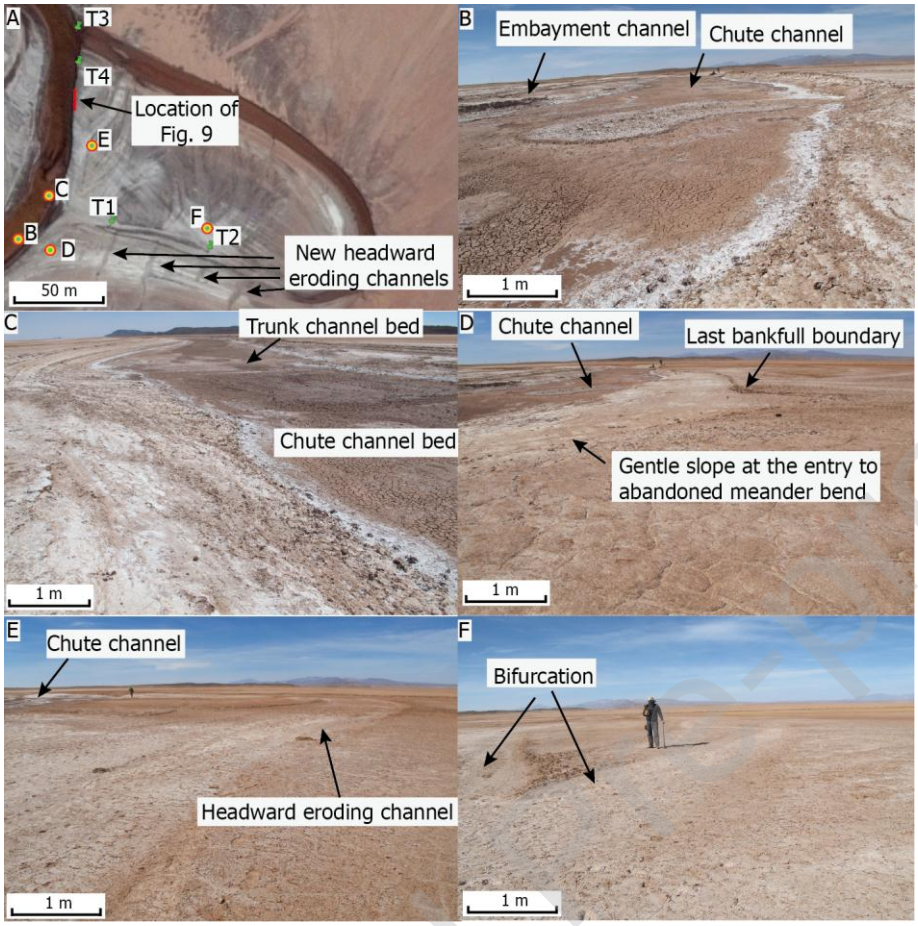

Fig. 6 Channel and abandoned bend development following chute cutoffs 1 and 2, visualised using high-resolution (<0.65 m) satellite imagery from November 2004 through 2010: (A-C) chute cutoff 1; (D-F) chute cutoff 2. In both cases, the new trunk channel can be seen to widen and develop more regular banklines over time.

Journal Pre-proof

Journal Pre-proof

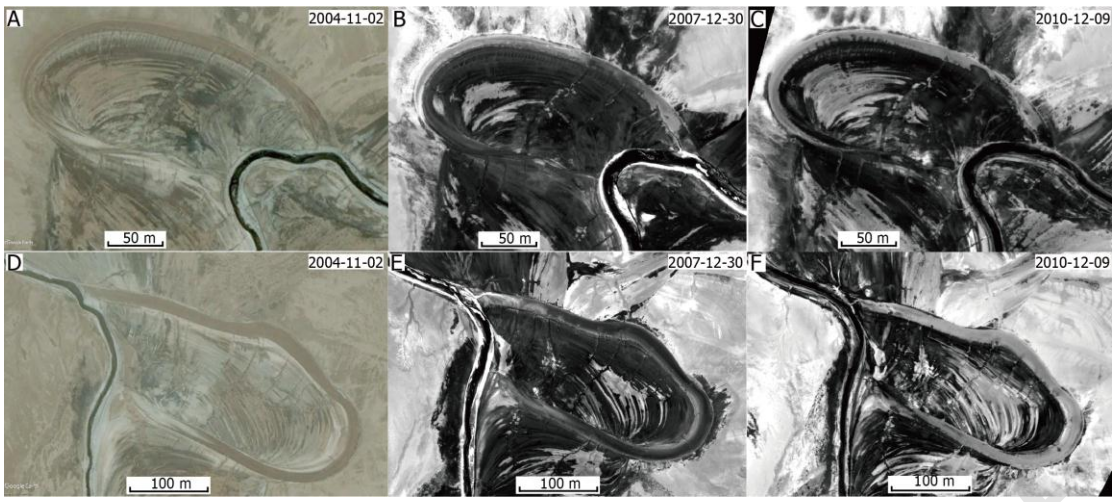

Fig. 7 (A) Modelled discharges for the study reach, derived by following the method of El-Hames (2012), with grey columns bracketing the timing of completion of chute cutoffs 1, 2 and 3; (B) Peak discharge events compared to ENSO MEI index; where the MEI index is greater than 0, it is an El Niño year and when the MEI is lower than 0, it is an La Niña year (https://www.esrl.noaa.gov/psd/enso/mei/table.html). Grey columns bracket the timing of completion of chute cutoffs 1, 2 and 3. (C) High-precision dGPS profile along part of the study reach (for location, see Fig. 1C).

Journal Pre-proof

Journal Pre-proof

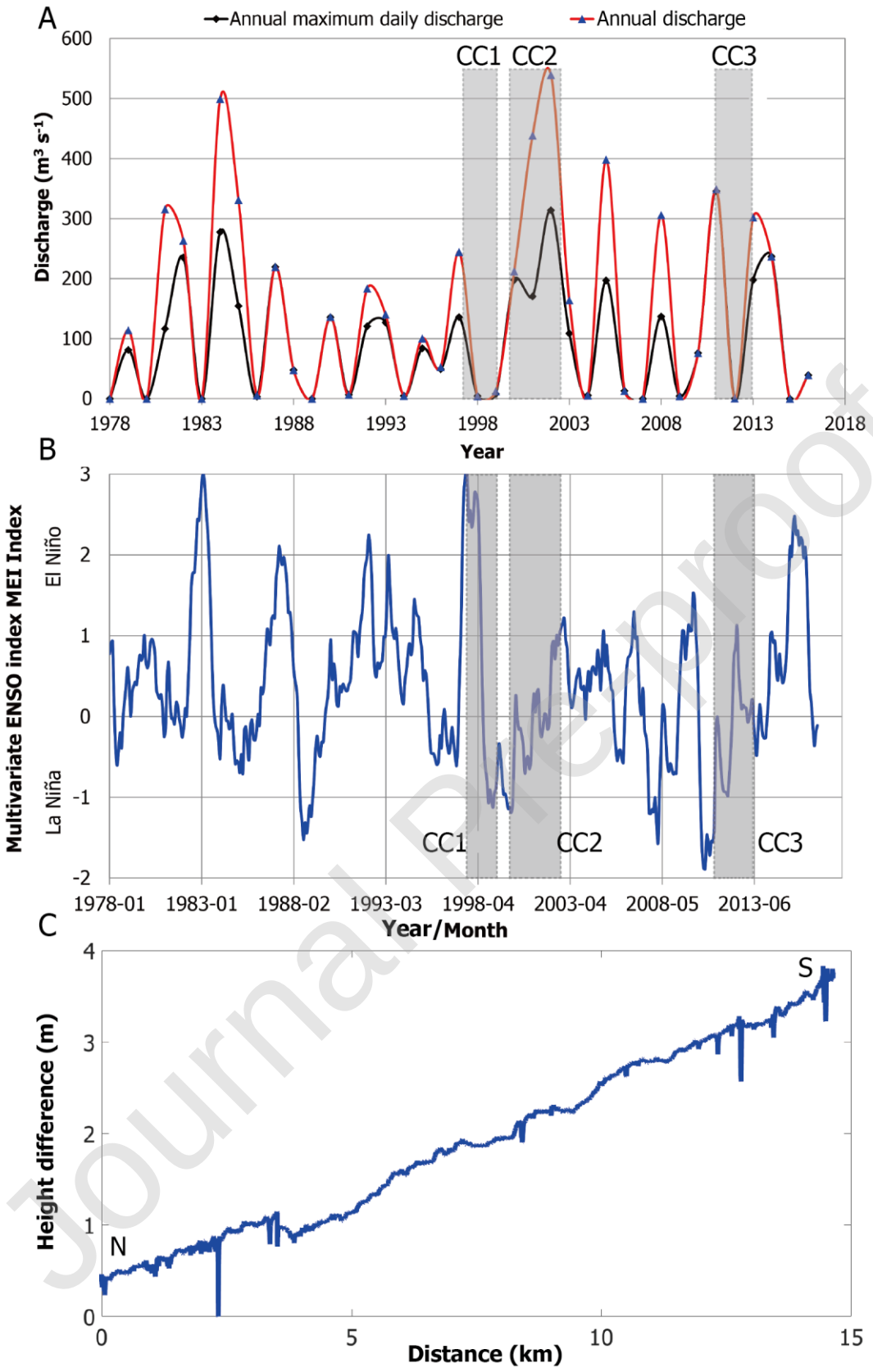

Fig. 8 Cumulative percentage grain-size curves for samples from CC3 with the median (black) and the median absolute deviation (dashed lines). See Fig. 5A for the location of

Journal Pre-proof

sample sites (trenches T1-T4).

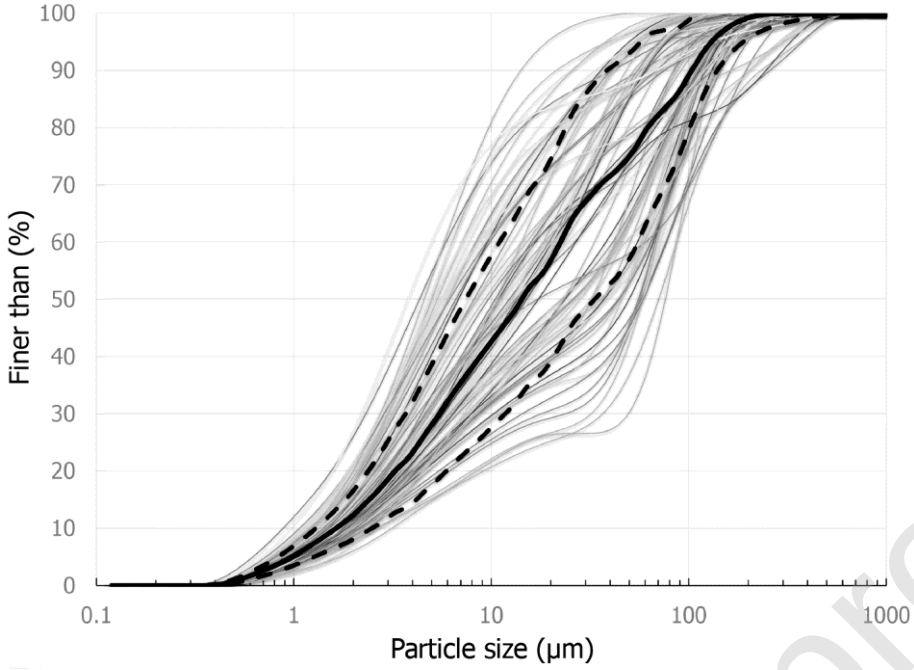

Fig. 9 Panoramic photograph of the accretionary terrain exposed along chute channel 3 (flow direction from right to left) and interpretation sketch (for location see Fig. 5A, and for scale, see the notebook of 20 cm length).

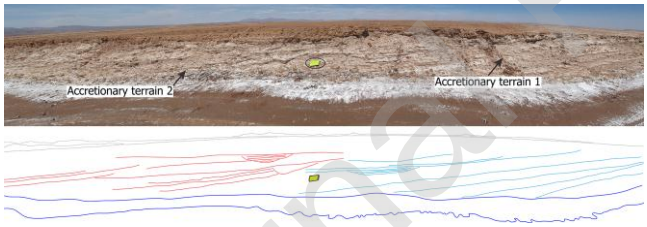

Fig. 10 Net erosion (area in m^2) along the study reach for various timeframes between 2004 and 2016, compared to modelled peak daily discharges for events >50 m^3s^{-1}, as derived by following the method of El-Hames (2012).

Journal Pre-proof

Journal Pre-proof

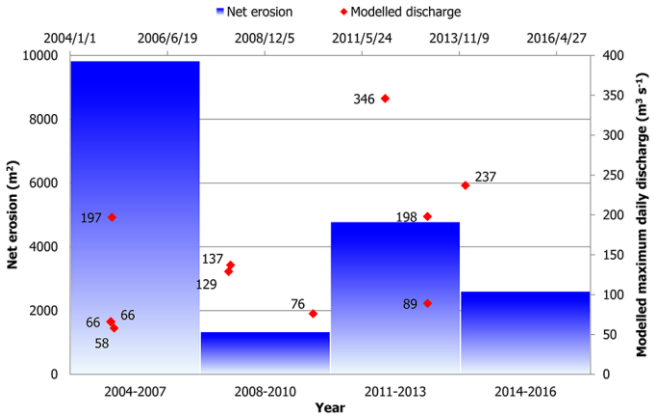

Table 1 Information regarding the high-resolution satellite imagery used in this study.

Type	Catalog ID	Acq. date	Avg. off nadir angle	Avg. target azimuth	Sensor
Quick Bird-02 (GoogleEarth)	10100100035DE200	Nov 2, 2004	8°	293°	QB02
Worldview-02	1020010001455700	Dec 30, 2007	17°	85°	WV01
	10300100084D5600	Dec 9, 2010	13°	173°	WV02
Pléiades	DS_PHR1B_201307131443591_SE 1_PX_W067S21_0310_02391	Jul 13, 2013	16°	33°	PHR1B
	DS_PHR1B_201603011443021_FR 1_PX_W067S21_0310_02408	Mar 01, 2016	11°	69°	PHR1B
	DS_PHR1B_201811021435528_FR 1_PX_W067S21_0216_05943	Nov 02, 2018	26°	80°	PHR1B

Table 2 Morphometrics of the 22 abandoned meander bends and chute cutoffs in the study reach.

Ratio of abandoned bend length to chute channel length		Angle (°) of divergence between channel-belt axis (chute channel) and upstream limb of abandoned bend	
Mean	4	Mean	98
Std. dev.	1.1	Std. dev.	16.9
Max.	6.2	Max.	142.4
Min.	2.2	Min.	74.6

Journal Pre-proof

Journal Pre-proof

Table 3 Morphometric and hydraulic parameters for chute channel 3 (2013 and 2016) and the former trunk channel around the abandoned bend (2013 only).

Parameter	Chute channel 2013	Chute channel 2016	Former trunk channel 2013
Channel width (m)	13.4	19.5	27.4
Bankfull discharge (m^3/s)	16.9	31.2	54.8
Specific stream power (W/m^2)	3.5	4.5	5.6

Journal Pre-proof